Polarization analysis and microstructural characterization of SOFC anode and electrolyte supported cells

Lanzini A., Leone P., Santarelli M., Asinari P., Calì M.

Dipartimento di Energetica. Politecnico di Torino. Corso Duca degli Abruzzi 24, 10129 Torino (Italy)

Abstract

The paper deals with the testing of performances of SOFC planar cells having as mechanical support either the anode or the electrolyte. Polarization traces at different temperature and hydrogen flow have been drawn to assess the electrochemical behavior and the limiting polarization factors of anode-supported and electrolyte-supported cells.

The experimental data from polarization tests has then been summarized and analyzed through a parameter estimation technique, which allowed us to compare the performances of each cell throughout some defined macroscopic parameters, each one being referred and distinctive of a certain polarization overvoltage occurring during a SOFC operation.

SEM and optical micrographs have been also collected in order to characterize the fine microstructure of the tested cells, and to discuss the macroscopic polarization results with reference to the microstructure.

Introduction

In 2006 Politecnico di Torino, joint with FN Nuove Tecnologie e Sistemi Avanzati S.p.A., has started a project named PFHC (Poly Fuel Hot Cell). The aim of the project is the design, production and experimental analysis of single solid oxide fuel cells of planar geometry, to be used in small stacks.

The main ongoing activities include: (i) manufacturing of anode-supported cells with different techniques for the deposition of the thin component layers (electrolyte and cathode) and with different electronic and ionic materials, pointing towards intermediate temperature operation (Figure 1); (ii) modeling and design of a single planar SOFC; (iii) experimental analysis and characterization of the cells in the High Quality Laboratory (LAQ) IN.TE.S.E., of the Dipartimento di Energetica of Politecnico di Torino; (iv) modeling and design of a SOFC stack, with particular attention to the reactants distribution system, to the cell interconnections and to the sealing material and design.

Figure 1. Industrial tape-caster machine for preparation of SOFC anode supports installed at FN Nuove Tecnologie e Sistemi Avanzati S.p.A.

In this paper, a performance evaluation of planar circular-shaped seal-less SOFC cells of different structure was performed, with an outline of the limiting factors at reduced temperature. The characterization was performed by taking V-I measurements over a range of temperatures between 640°C and 840°C. The dependence of the cell performance on the various polarization contributions was rationalized on the basis of an analytical model, through parameter estimation on the experimental data, to obtain some defined macroscopic parameters of the polarization overvoltage occurring during operation. SEM and optical micrographs have been also collected in order to characterize the fine microstructure of the tested cells, and to discuss the macroscopic polarization results with reference to the microstructure.

Figure 2. Experimental setup for the testing of planar cells

Results and analysis of the polarization curves on anode-supported and electrolyte-supported cells

In the test facility installed at LAQ IN.TE.S.E. in Politecnico di Torino (Figure 2) several polarization test on InDEC® anode-supported cells (ASC1 and ASC2, differing for the cathode design and material) and on electrolyte-supported cells (ESC2) were undertaken. The ASC1 design consists of a 500-520 µm NiO/8YSZ anode support, a 4-6 µm 8YSZ electrolyte, a 14-16 µm LSM/8YSZ

cathode active layer and a 18-20 µm pure LSM current collector layer. The ASC2 has the same anode and electrolyte but the cathode is a single 40-45 µm layer made of LSCF; between it and 8YSZ layer there is a protective layer of YDC to prevent the formation of undesired compounds and to reduce the thermal stresses due to the different values of thermal expansion coefficient of electrolyte and cathode materials.

Finally, the ESC2 cell consists of a 40 µm NiO/GDC anode active layer, a 90-100 µm 3YSZ supporting electrolyte layer and a cathodic double-layer identical to that of the ASC1.

The cells' active area was of 47 cm^2. The aim of our experimental sessions was to understand the main limiting factors in each type of cell and establish a testing protocol for unsealed planar cells.

In Figure 3 the electrochemical behaviour of the different cell types at the intermediate temperature of 800°C are reported. The better performances of the ASC cells are evident if compared to the ESC2 cell type.

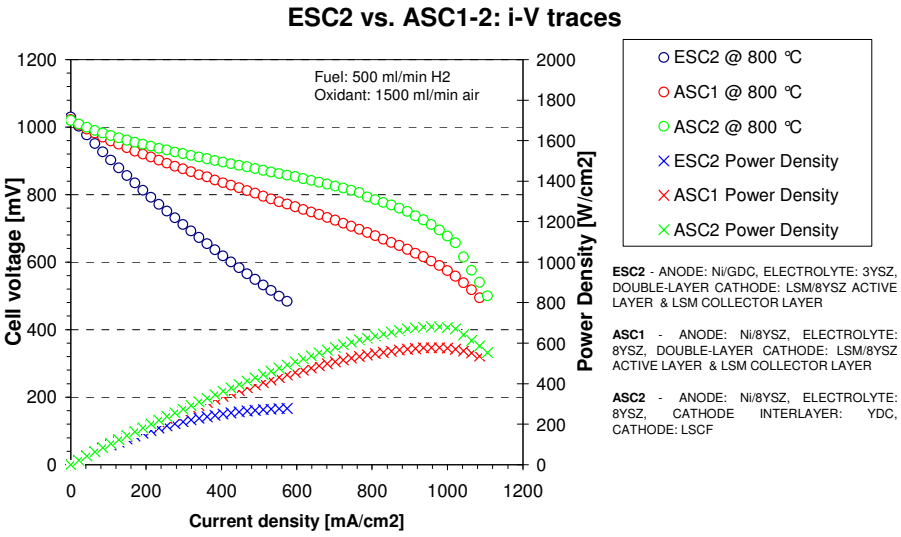

Figure 3. Polarization curves for ASC1, ASC2 and ESC2

As already mentioned, the ESC2 cell has the same double-layer cathode structure of the ASC1, and an anode layer with a very fine composite and graded microstructure. So the really limiting feature of the ESC2 is the thickness of its electrolyte layer and the reduced conductivity of 3YSZ at temperature below 900-1000°C.

The comparison between the ASC1 and ASC2 behaviour shows that the latter type is even better performing because of the use of a MIEC cathode [1], namely LSCF: this material provides a high charge-transfer rate for the oxygen reduction and a really extended TPB region, acting also as a good electronic charge collector.

In Table 1 the measured maximum power density (MPD) for each type of cell at different temperatures are reported.

Table 1. Maximum Power Density (MPD) of the tested cells (@500 ml/min H_2)

ASC1	MPD [W/cm^2]
Test @ 740°C	0.43
Test @ 800°C	0.58
Test @ 840°C	0.65

ASC2	MPD [W/cm^2]
Test @ 650°C	0.35
Test @ 740°C	0.61
Test @ 800°C	0.68
Test @ 840°C	0.77
ESC2	**MPD [W/cm^2]**
Test @ 740°C	0.13
Test @ 800°C	0.23
Test @ 840°C	0.35

In Figure 4 the experimental OCV is also compared at various temperatures. The ESC2 shows a slightly better open-circuit voltage, probably due to the thickness of the electrolyte layer which provides a good tightness between the reactant gases. In the ASC1-2 the very thin electrolyte layer can have some pinholes in it (as seen in Figure 4) which can decrease the OCV because of an internal cross-over of the reactants gases from the cathode to the anode side. This phenomenon decreases the cell Nernst potential. However the main reason for the discrepancy from the theoretical open circuit voltage and the experimental one is probably due to the back flow of inlet air in the anode side. In this way part of the hydrogen fuel burns at the external radius of the cell and the effective fuel molar fraction is somewhat lower than at the inlet radius.

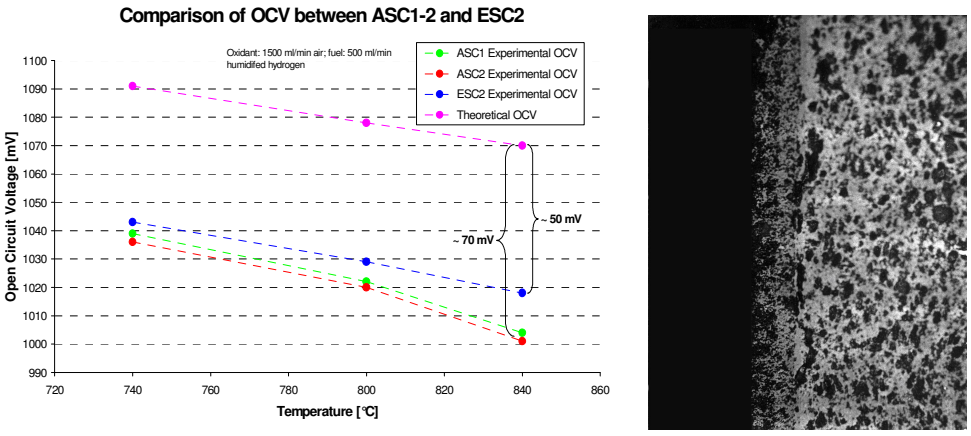

Figure 4. (right) OCV comparison between the different cell types; (left) optical image of the cross-section of an ASC1 cell

Microstructural characterization of tested cells

The cell under consideration in this paper have been characterized through a ZEISS Scanning Electron Microscope and an optical microscope. ASC1 and ASC2 are both anode supported cells, being a Ni/8YSZ cermet the anode support.

The significant feature of the ASC1 cell is the cathode double layer. The outer layer is the cathode current collector (Figure 5). It has the function of collecting and gathering out of the electrode the electrons coming from the oxygen electrochemical reactions. It also has a certain porosity to let the oxygen flow pass thorough it and reach the active layer. This layer (which is the inner one, closer to the electrolyte) is made of YSZ (ionic phase)

and LSM (electronic phase); the composite structure should be very effective in increasing the three-phase-boundary for the electrochemical reduction of the oxygen.

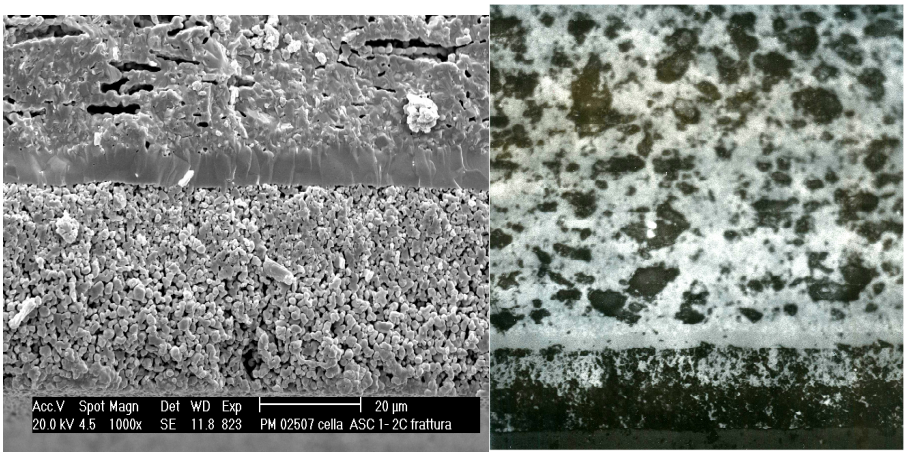

Figure 5. (right) SEM microscopy of ASC1 cell; (left) optical image of the same region; for both images, from top to bottom: Ni/8YSZ anode support, 8YSZ thin electrolyte, LSM/8YSZ cathode active layer, LSM cathode current collector

The ASC2 cell has completely different cathode design and material. In Figure 6, it can be seen that the cathode electrode consist of just one layer of a very fine structure. The material used is LSCF, which has ambivalent electrical properties, that means it is able to conduct at the same time ions and electrons; so it is a very active material for the oxygen electrochemical reduction (it increases the three phase boundary). Its chemical compatibility at high temperatures with 8YSZ is not very good, so an extra electrolyte interlayer (YDC) has been put between the LSCF cathode and the conventional 8YSZ electrolyte. Doped-ceria is a very fine ions conductor, anyway the interlayer thickness is very reduced to avoid additional ohmic resistance internal to the cell.

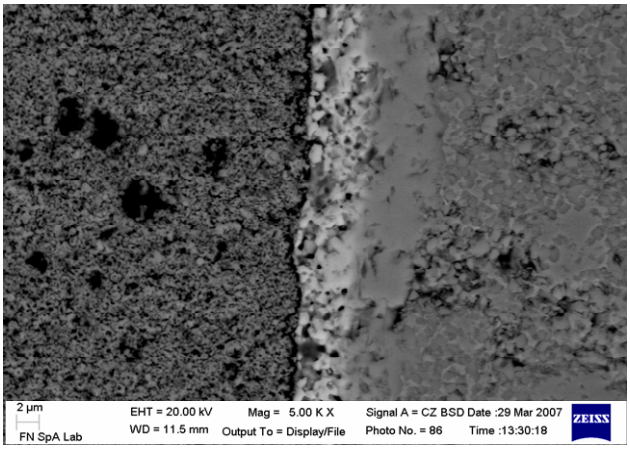

Figure 6. SEM microscopy of an ASC2 cell; from top to bottom: Ni/8YSZ anode support, 8YSZ thin electrolyte, YDC protective interlayer, LSCF cathode active and collecting layer

The ESC2 cell form InDEC consists of a thick and dense 8YSZ electrolyte as supporting layer (Figure 7). The anode electrode is made of Ni-GDC, and has porosity

graded microstructure. In particular, three different layers can be seen at the top of Figure 4: the first most external and irregular layer has a coarser structure to let the hydrogen flow into the cell, then follows a finer and probably already active layer, and finally a very thin and less porous active interlayer (about 4 microns of thickness) that interfaces the electrolyte. This very structured anode should be very effective for the hydrogen reactions activation.The cathode is the same of the ASC1 cell.

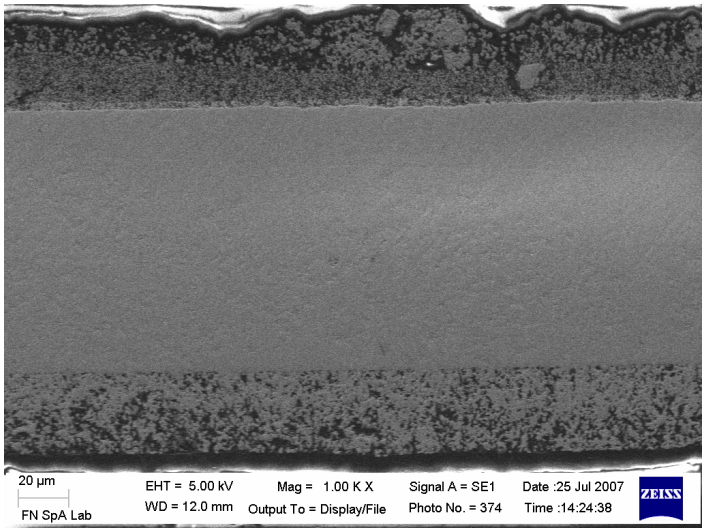

Figure 7. SEM micrograph of an ESC2 cell section; (top) graded Ni-GDC anode layer , thick 8YSZ electrolyte, LSM/8YSZ & LSM double layer

Parameter estimation from the experimental data

The regression model of the polarization curve used for the parameter estimation of the experimental data is described as follows:

$$V = E(T,p) - \eta_{activation} - \eta_{ohmic} - \eta_{concentration} \tag{1}$$

- *Activation overvoltage* [2,5]:

$$\eta_{activation} = \frac{R \cdot T_{cell}}{1.4 \cdot F} \cdot \log\left(\frac{i}{i_{0,cat}}\right) \tag{2}$$

- *Ohmic overvoltage:*

$$\eta_{ohmic} = R_{ohm,tot} \cdot i_c \tag{3}$$

- *Concentration overvoltage* [3]:

$$\eta_{concentration} = -\frac{R \cdot T_{cell}}{2 \cdot F} \cdot \log\left(1 - \frac{i}{i_{as}}\right) \tag{4}$$

- *Total cell polarization model*:

$$V(i) = OCV - i \cdot R_{ohm,tot} - \frac{R \cdot T_{cell}}{1.4 \cdot F} \cdot \log\left(\frac{i}{i_{0,cat}}\right) + \frac{R \cdot T_{cell}}{2 \cdot F} \cdot \log\left(1 - \frac{i}{i_{as}}\right) \tag{5}$$

The estimated parameter are the total ohmic cell resistance $R_{ohm,tot}$, the cathode exchange current density $i_{0,cat}$ and the anode limiting current density i_{as}. In the adopted electrochemical model the cathodic concentration polarization is neglected for all the cells parameter estimation since the diffusion path of the oxidant flow through the cathode is very short compared to that of the hydrogen flow through the anode support. It is also neglected the activation polarization of the anode since the electrocatalytic activity of Ni is known to be at least one order of magnitude higher than the one of the cathode materials.

In Figure 6 and 7 the results of the fitting of the experimental results by the electrochemical model described by eq. (5) are shown.

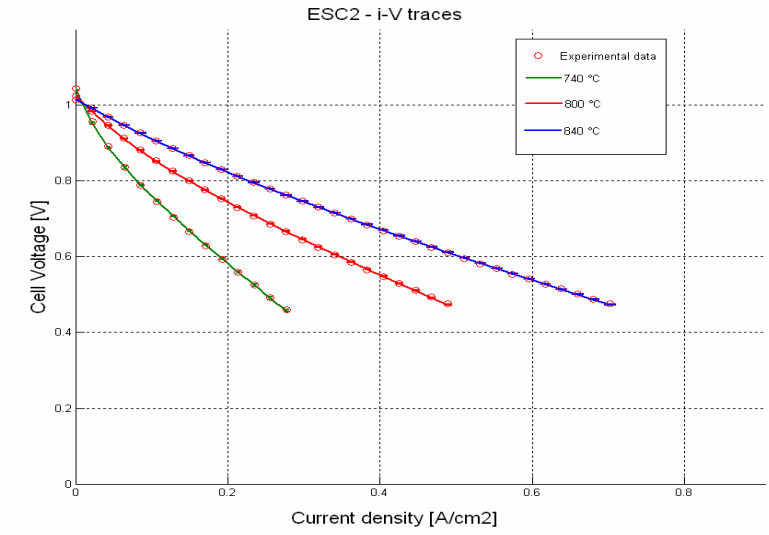

Figure 6. Example of polarization curves fitting for an ESC2 cell through the electrochemical model described by eq. (5)

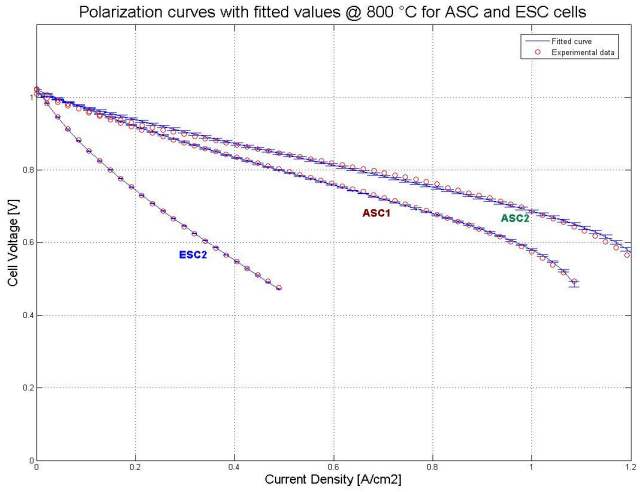

Figure 7. Experimental and fitted polarization curves for all the cell types investigated in this paper (ASC1-2 & ESC2)

Table 2. Parameter estimation of the tested cells

ASC1 cell			
Temperature [°C]	**i_{as} [A/cm^2]**	**$R_{ohm,tot}$ [ohm*cm^2]**	**$i_{0,cat}$ [A/cm^2]**
740	0.954 ± 0.0445	0.469 ± 0.0073	0.037 ± 0.0080
800	0.978 ± 0.0059	0.235 ± 0.0041	0.071 ± 0.0020
840	1.097 ± 0.0064	0.097 ± 0.0080	0.145 ± 0.0112
ASC2 cell			
Temperature [°C]	**i_{as} [A/cm^2]**	**$R_{ohm,tot}$ [ohm*cm^2]**	**$I_{0,cat}$ [A/cm^2]**
650	1.188 ± 0.1540	0.500 ± 0.0113	0.037 ± 0.0012
740	1.052 ± 0.0056	0.173 ± 0.0103	0.140 ± 0.0120
800	1.070 ± 0.0067	0.083 ± 0.0105	0.167 ± 0.0108
840	1.197 ± 0.0024	0.045 ± 0.0145	0.210 ± 0.0396
ESC2 cell			
Temperature [°C]	**i_{as} [A/cm^2]**	**$R_{ohm,tot}$ [ohm*cm^2]**	**$i_{0,cat}$ [A/cm^2]**
740	-	1.361 ± 0.0233	0.010 ± 0.0007
800	-	0.737 ± 0.0053	0.027 ± 0.0007
840	-	0.536 ± 0.0026	0.063 ± 0.0015

In Table 2 the results of the parameter estimation are summarized. From the ESC2 polarization curves it has not been possible to determine the limiting anodic current density since the cell voltage reached the critical testing point of 400 mV far before the concentration polarization arises, that is usually at high current density. Nevertheless, the ESC2 cell has very thin anode graded electrode and diffusion of the reactants should not be a limiting factor.

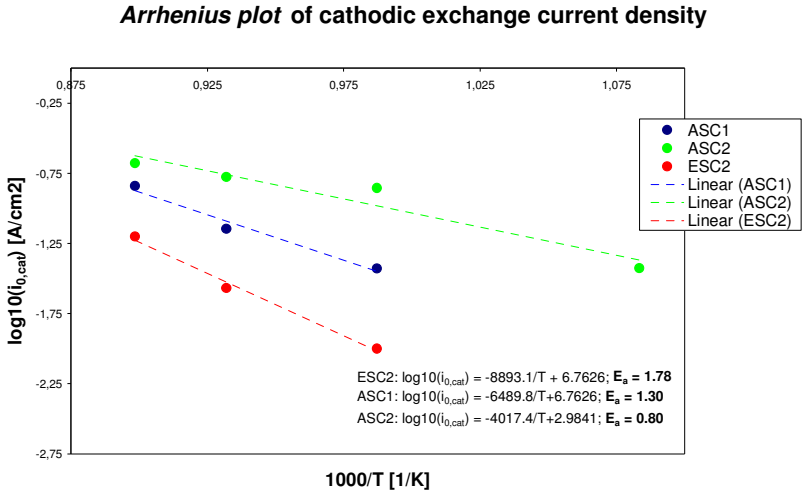

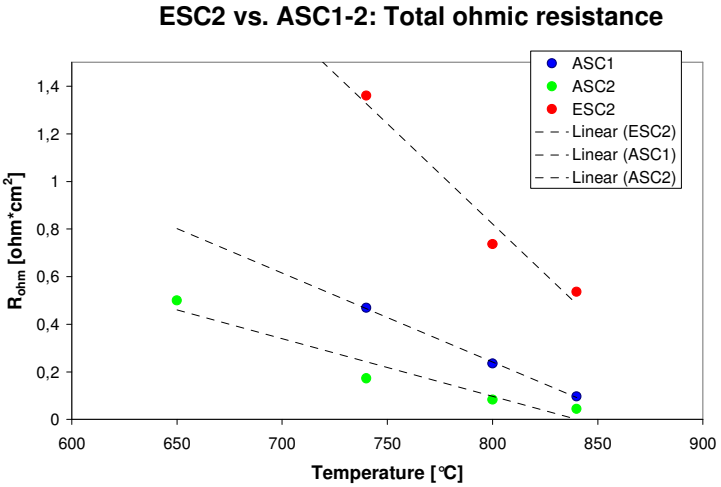

Figure 8. Plots of the estimated a) $i_{0,cat}$ and b) $R_{ohm,tot}$

From the plots in Figure 8 the better performances of ASC cells within respect of the ESC2 in terms of both ohmic resistance and activation polarization is outlined. In particular, the ASC2 shows the best results; its cathodic exchange current has the lowest activation energy, that means it has a less dependent behavior against temperature; basically, the activation polarization, as the operative temperature goes down, increases slower for the ASC2 cell compared to that of the other two cell types. This is true also in terms of ohmic resistance. Probably, this due to the LSCF cathode, which provides other than better electrochemical kinetics also good electronic collecting properties. From the graph in Figure 8b, it is clear that the liming factor in the electrolyte-supported cells is ohmic drop across the electrolyte layer.

To further analyze the high ohmic polarization of ESC2, in Table 3 the ohmic resistance of the electrolyte layer is evaluated form available literature data and this value is compared to the total ohmic resistance estimated from the experimental data ($R_{ohm,tot}$). The $R_{ohm,3YSZ}$ is calculated from the conductivity of the material constituting the electrolyte of the cell; the inverse of the conductivity multiplied by the electrolyte thickness gives the ohmic ASR due to this component (the $R_{ohm,3YSZ}$) at a certain operating temperature. The empirical correlation for the 3YSZ electrolyte conductivity is reported in eq. (6):

$$\sigma_{3YSZ} = \frac{\sigma_0}{T} \cdot \exp\left(\frac{E_a}{R \cdot T}\right) \text{ [S/cm]} \qquad (6)$$

$\sigma_0 = 2.0374 \cdot 10^5$ [S/cm]

$E_a = 0.83$ [kJ/mol/K]

It is confirmed that the very high ohmic resistance of the ESC2 cells is due to the limited conductivity of 3YSZ at intermediate temperature and to the thickness of the electrolyte layer.

From Table 3 it is also shown that as temperature increases, the ohmic contribution for the layers other than the electrolyte becomes somewhat higher, reducing so the overall share due to the electrolyte layer.

Table 3. Electrolyte vs total ohmic resistance in ESC2 cell (electrolyte thickness 100 μm)

ESC2 cell			
Temperature[°C]	$R_{ohm,tot}$ [ohm*cm^2]	$R_{ohm,3YSZ}$ [ohm*cm^2] [4]	$R_{ohm,3YSZ}$ [%]
740	1.361	0.947	70%
800	0.737	0.578	78%
840	0.536	0.429	80%

Conclusions

From the tests performed and analyzed here it appears clear that at intermediate temperatures the best cell type design is the anode-supported one. Within this cell typology design, the cathode material and design has a great importance in improving the electrochemical performances. The ASC2 with a MIEC LSCF cathode shows not only an higher estimated $i_{0,cat}$, that means reduced activation polarization, but also a lower total $R_{ohm,tot}$, probably due to the good current collecting properties of the cobaltite-ferrite cathode.

References

[1]. Jiang S.P., Wang W., Novel structured mixed ionic and electronic conducting cathodes of solid oxide fuel cells. Solid State Ionics 176 (2005) 1351-1357.

[2]. Costamagna P., Honegger K., Modelling of Solid Oxide Heat Exchanger Integrated Stacks and simulation at high fuel utilization, J. Electrochemical Soc. 145 (1998) 3995-4007.

[3]. Kim J., Virkar A.V., Fung K.Z., Metha K., Singhal S.C., J. Electrochemical Soc. 146 (1999) 69-78.

[4]. Sukhvinder P.S. Badwal, Fabio T. Ciacchi, Kristine M. Giampietro, Analysis of the conductivity of commercial easy sintering grade 3 mol% Y2O3–ZrO2 materials, Solid State Ionics 176 (2005) 169-178.

[5]. Costamagna P., Costa P., Antonucci V., Micro-modelling of solid oxide fuel cell electrodes, Electrochimica Acta 43 (1998) 375-394.